1977A&A....59...27I

Astron. Astrophys. 59, 27—41 (1977)

ASTRONOMY AND ASTROPHYSICS

Aperture Synthesis Observations of Galactic H II Regions

IV. New Observations of H II Regions around $l = 111°$

F. P. Israel

Sterrewacht, Huygens Laboratorium, Wassenaarseweg 78, Leiden 2405, The Netherlands

Received September 22, 1976

Summary. New observations at λ 6 cm and re-examination of old λ 21 cm observations confirm and extend the conclusions drawn earlier from WSRT data (Israel et al., 1973). In the Cas-Cep section of the Perseus Arm a loose OB association appears to be forming; formation of stars occurs in subgroups, at the outer edge of neutral clouds.

The area is the site of active star formation, with high density compact H II components in S 156, S 157, S 158 and S 159.

The available information on S 156 and S 158 is consistent with a model originally applied to the Orion nebula (Zuckerman, 1973; Balick et al., 1974), in which model an early type star ionizes a neutral cloud from outside; ionized gas streams away from the resulting ionization front. Both S 156 and S 158 are viewed almost edge-on. A comparison of optical and radio observations shows clumping factors of 2–10 for S 156, 10–90 for S 158 and around 2 for S 162.

Key words: radio observations — star formation — H II regions

Introduction

This paper is fourth in a series dealing with high resolution observations of galactic H II regions using the Westerbork Synthesis Radio Telescope (WSRT). In the first paper of this series (Israel et al., 1973; Paper I) six H II regions in the Cassiopeia-Cepheus region of the Milky Way were studied at a wavelength of 21 cm. At an assumed distance of 3.5 kpc, our λ 21 cm synthesized beam corresponds to a linear resolution of about 0.4 pc. This proved to be insufficient to resolve the small-scale structure in S 158 and barely sufficient to show any structure at all in the regions S 156, S 157 and S 159. It was therefore decided to study all regions from Paper I also at a wavelength of 6 cm, where the WSRT has a synthesized halfpower beamwidth of 7″, yielding a linear resolution of about 0.1 pc at the distance of the H II regions. Also, by cleaning and restoring (Högbom, 1974; Harten, 1976) the old λ 21 cm maps additional and better information was obtained.

In Paper I we already gave the radial velocities of S 156–S 162, as well as information on previous radio observations. Since then, new information has become available, which I summarize in Tables 1 and 2.

The radio observations from Table 1 and from Table 3 in Paper I define optically thin, thermal spectra. The only significantly different spectrum is that of S 162. The cause of this was discussed by Johnson (1971) and by us in Paper I.

II. Observations

The WSRT is described in detail by Baars and Hooghoudt (1974), and Casse and Muller (1974), Högbom and Brouw (1974) gave a description of the principles of operation, reduction and calibration. In Table 3 I give the observing log. All λ 6 cm observations were made with interferometer spacings ranging from 36 m to 1404 m with increments of 72 m. At λ 6 cm, the primary beam has a width at half power of 12′. The synthesized beam measures 7.2×7.2 cosec δ arc sec. The (1σ) r.m.s. noise is 1.3 m.f.u. per synthesized beam area per 12 h period. All sources were observed during 1×12 h, with the exception of G 110.25 that was observed for 7 h. The structure of the extended sources (like S 158 and S 162) was distorted by internal interference, and by the lack of spacings shorter than 36 m. Moreover, the early λ 21 cm observations of S 156/G 110.25 + 0.01 and S 157 were distorted by incomplete hour angle coverage and other instrumental effects. Therefore I used the clean method (Högbom, 1974; Harten, 1976).

All sources were restored onto the residual maps with an artificial beam of the same size as the actual beam, but lacking sidelobes. In order to study small-scale structure in S 158, I also made a λ 6 cm map of this source containing only spacings longer than 250 m (4167 λ). The contour maps of Figures 10 and 11 are based on this cleaned and restored map. The observational results are

© European Southern Observatory • Provided by the NASA Astrophysics Data System

1977A&A....59...27I

Table 1. Previous radio observations[a]

Object	Frequency (MHz)	HPBW (arcmin)	Flux-density (f.u.)	Reference
(1)	(2)	(3)	(4)	(5)
S 156	408	4.2 × 114	1.4	Fanti et al. (1974)
	1410	4 × 22	2.15	Kazès et al. (1975)
	2695	2.2 × 11	2.13	Kazès et al. (1975)
	2695	5.2	2.2±0.3	Terzian et al. (1973)
	4850	1.5 × 7	2.0	Kazès et al. (1975)
	7850	4.3	2.3±0.1	Goad (unpublished)
	8000	4.4	2.2	Johnson (1974b)
	15000	2.2	1.8±0.1	Johnson (1974)
	31000	3.7	3.9±0.5	Johnson (1974b)
S 157 A+B	1416	4 × 22	0.56	Kazès et al. (1975)
	4850	1.5 × 7	0.62	Kazès et al. (1975)
S 158	408	4.2 × 114	22.0	Fanti et al. (1974)
	2695	5.2	25.7±4.0	Terzian et al. (1973)
	2695	0.18 × 0.21	15 ±5	Martin (1973)
	7800	4.2	23.3±2.3	Lada and Chaisson (1973)
	31000	3.7	8.2±0.2	Johnson (1974b)
	85000	1.3	4.3±0.9	Johnson (1974b)
S 159	2695	5.2	2.6±0.4	Terzian et al. (1973)
S 162	2695	5.2	15.1±2.5	Terzian et al. (1973)
	5000	11	13.7±0.6	Barlow et al. (1974)

[a] See also Table 3, Paper I

Table 2. Radial velocities

Name	Line	Velocity V_{LSR} (km s^{-1})		Reference
(1)	(2)	(3)		(4)
S 156	Hα	−50.0		Georgelin (1975)
	CO	−51.8		Blair et al. (1975)
	H_2CO	−52		Höglund and Gordon (1973)
	OH diffuse	−52		Höglund and Gordon (1973)
	CO	−51.5		Dickinson et al. (1974)
S 157	Hα	−37.7		Georgelin (1975)
	Hα	−46		Deharveng (1974)
S 157 Knot	Hα	−46		Deharveng (1974)
	CO	−46		Dickinson et al. (1974)
S 158[a]	Hα	−59.6		Georgelin (1975)
	H 94α	−59.8		Lada and Chaisson (1973)
	H 109α	−60.6		Reifenstein et al. (1970)
	OH maser	−54.8	−60	Wynn-Williams et al. (1974)
	H_2O maser	−53	−62	Cato et al. (1975)
S 159	CO	−56		Dickinson et al. (1974)
	CH	−54		Hjalmarson et al. (1975)
S 162	Hα	−46		Deharveng (1973)
	Hα	−45.2		Georgelin (1975)

[a] See also Table 7, this Paper

Table 3. Observing log

Fields	Date	Duration	Coordinates fieldcenter α (1950.0)	δ (1950.0)
(1)	(2)	(3)	(4)	(5)
S 156	May 1973		$23^h03^m05^s$	59°58′48″
G 110.25	Nov 1972		$23^h05^m00^s$	59°58′59″
S 157	Jan 1973		$23^h13^m59^s$	59°46′01″
S 158	July 1973		$23^h11^m24^s$	61°13′48″
S 159	July 1973		$23^h13^m24^s$	60°50′24″
S 162	May 1974		$23^h18^m43^s$	60°55′48″

listed in Table 4. In Table 5 I give other sources found in the observed fields.

In Table 4, column 1 gives the name of the component, columns 2, 3, 4 and 5 give equatorial and galactic coordinates respectively, columns 6 and 7 contain the observed λ21 cm and λ6 cm flux densities, and column 8 gives the equivalent gaussian angular diameter, corrected for finite beamsize. Note that the λ21 cm flux densities in column 6 are revised values; they are sometimes different from those in Paper I.

Flux densities were determined by planimetering the contour maps, and sometimes checked by adding the delta functions found by the clean procedure. Positions and sizes were determined from contour maps. In these maps, 1 m.f.u. per synthesized beam area corresponds to a brightness temperature $T_b = 1.2 \sin\delta\, K$. In Table 5, column 1 gives a sequence number, column 2 gives the name of the field in which the source was found, columns 3 and 4 give equatorial coordinates, and columns 5 and 6 give peak flux densities. Both position and flux density were determined by the standard search programma (Van Someren Greve, 1974); only those marked with an asterisk I determined by eye estimate from contour maps. The flux densities are all corrected for the decrease of the primary beam sensitivity towards the edge of the field.

III. Results

1. *Physical Parameters*

From the observed parameters in Table 4 I derived model physical parameters using the equations given by Mezger and Henderson (1967). In order to obtain a lower limit for

© European Southern Observatory • Provided by the NASA Astrophysics Data System

1977A&A....59...27I

Table 4. Observed parameters

Name	Right ascension (1950.0)	Declination (1950.0)	Gal. long. l	Gal. long. b	Flux density S_{1415} (m.f.u.)	S_{4995} (m.f.u.)	Equivalent gaussian diameter (arc sec)
(1)	(2)	(3)	(4)	(5)	(6)	(7)	(8)
S 156 A	$23^h03^m04^s.3$	59°58′33″	110.108	+0.048	{850}	585±50	5×12
B	23 03 05.4	59 58 20	110.108	+0.043		40±10	4
C	23 03 03.6	59 58 20	110.105	+0.045		35±10	4
Inner Envelope	23 03 04	59 58 22	110.11	+0.05	—	765±100	35
Outer Envelope	23 03 04	59 58 22	110.11	+0.05	1500	1000±150	90×75
G 110.25+0+01 A	23 04 16.1	60 00 09.6	110.256	+0.013	{50}	40±10	15×25
B	23 04 16.9	59 59 38.5	110.254	+0.005		15±5	11
Envelope	23 04 17.0	60 00 00	110.26	+0.01	50	—	70
S 157 A	23 13 59.1	59 46 06.4	111.30	−0.66	730	660±50	59×68
B	23 13 52.8	59 45 39.6	111.283	−0.663	130	105±20	4
C	23 13 50.9	59 45 18.2	111.277	−0.667	—	25±5	6×13
D	23 13 56.1	59 45 22.0	111.288	−0.670	—	20±5	6
G 111.2−0.8	23 13 00	59 36 00	111.21	−0.77	400±100	—	215
G 111.4−0.7	23 14 45	59 48 00	111.40	−0.67	675±150		320
G 111.5−0.6	23 15 25	59 52 00	111.50	−0.63	575±150	—	245
S 158 A 1	23 11 20.7	61 13 45	111.524	+0.819	{3150±750}	195±50	9
A 2	23 11 23.4	61 13 37	111.528	+0.814		355±75	4.5×33
A 3	23 11 22.7	61 14 01	111.529	+0.821		25±5	<4
A Envelope	23 11 22.0	61 13 45	111.53	+0.83		2000±500	54
B 1	23 11 21.2	61 13 01	111.521	+0.807	{600±200}	125±35	9
B 2	23 11 23.1	61 12 48	111.523	+0.802		400±100	4.5×48
G Total	23 11 37	61 11 59	111.54	+0.78	850	1400±200	7
G 1	23 11 37	61 11 59	111.54	+0.78	—	120±25	0.7[a]
G 2	23 11 36.80	61 11 59.3	111.543	+0.779	—	1300±200	8[b]
G 3	23 11 34.95	61 11 53.6	111.539	+0.779	—	20±10	3
Shell[c]	23 11 25	61 13 30	111.53	+0.81	18000	16000±2500	150
S 159 A	23 13 21.4	60 50 49.2	111.612	+0.374	800	1010±50	6
S 162 Total	23 18 30	60 55 40	112.23	+0.23	1150±175	1025±175	100×40
A 1 (Comet)	23 18 29.5	60 55 05	112.222	+0.221	360±90	310±90	20×35
A 2 (Bubble)	23 18 33	60 55 30	112.231	+0.226	790±150	715±150	85×30
B	23 18 49.5	60 57 00	112.271	+0.238	35±10	20±10	15×5
C Total	23 18 30	60 57 10	112.24	+0.25	610±200	665±200	70×110
C 1	23 18 39.0	60 57 10	112.252	+0.247	{100±30}	70±20	25
C 2	23 18 34.0	60 56 55	112.241	+0.247		55±20	30
C 3	23 18 32.5	60 57 40	112.242	+0.260		40±15	25
C Envelope	23 18 30	60 57 10	112.24	+0.25	510±200	500±200	70×110

[a] Based on a turnover frequency of 5 GHz with $S = 0.12$ f.u.
[b] Based on a turnover frequency of 2 GHz with $S = 1.4$ f.u.
[c] Including components D, E and F, but excluding components A, B, C and G (cf. Paper I)

the mass of unresolved objects I used the equation $M(M_\odot) \geqq 0.0026 S^{1.25}_{(\text{f.u.})} D^{2.5}_{(\text{kpc})}$ given by Matthews et al. (1973). The physical parameters of the compact objects S158G1 and S158G2 (see Sect. 5.4) are based on equations given by Mezger et al. (1967) for the case where the radio spectrum and the turnover frequency are known. The results are given in Table 6.

The model parameters describe cylindrical H II regions that consist of pure hydrogen at $T_e = 10^4$ K. The depth of the cylinder equals its diameter. The gas distribution is homogeneous, so that the clumping factor f is unity[1]. As a consequence, the listed values for the mass are upper limits; the actual mass scales with $f^{-1/2}$.

[1] The clumping factor f is defined as $\theta^3_{\text{total}}/\theta^3_{\text{clump}} \propto n_e^2/\langle n_e^2 \rangle$

2.1 S 156 = IC 1470

In Paper I we discussed the nebula as a just resolved bright radio peak and a surrounding low brightness envelope. In the new λ 21 cm map, the envelope appears larger than in the old one (Fig. 1). The new λ 6 cm observations show an appreciably more complicated structure (Fig. 2). There is a good qualitative correspondence between the λ 6 cm radio map and short exposure optical photographs (cf. Deharveng, 1974 and Barlow et al., 1974). For comparison, I reproduce the Hα photograph, adapted from Deharveng (1974) as Figure 3.

The similarity of the radio and optical pictures of the nebula implies that the extinction varies smoothly over the nebula.

© European Southern Observatory • Provided by the NASA Astrophysics Data System

1977A&A....59...27I

Table 5. Other sources found in the observed fields

Number	Field	Right ascension (1950.0)	Declination (1950.0	Flux density	
				S_{1415} (m.f.u)	S_{4995} (m.f.u.)
(1)	(2)	(3)	(4)	(5)	(6)
1	S 156	$23^h01^m53^s.6$	59°43′59″	40	—
2*		23 03 10.9	59 44 10	20	—
3		23 04 15.7	60 05 39	42	—
4		23 04 53.0	59 49 00	10	6
5		23 05 12.1	60 03 02	71	20
6		23 05 40.0	59 53 52	22	—
7		23 07 13.7	59 39 52	46	—
8*	S 158	23 08 56.0	61 15 10	70	—
9		23 09 02.8	61 02 59	46	—
10		23 09 27.8	61 07 34	70	—
11		23 09 47.6	61 12 56	53	—
12		23 10 32.1	61 28 11	52	—
13	S 157	23 10 43.5	59 22 37	660	—
14*	S 158	23+1 00.0	61 40 18	60	—
15		23 11 01.4	60 53 50	290	—
16*	S 157	23 11 39.3	59 23 27	40	—
17*		23 12 12.0	59 22 40	29	—
18		23 13 19.0	59 21 16	45	—
19*	S 158	23 13 26.9	61 33 35	60	—
20*	S 157	23 13 35	59 36 18	25	—
21		23 13 38.5	59 50 55	20	<5
22		23 13 40.2	59 53 10	17	<9
23*		23 13 48.0	59 36 15	15	—
24*	S 158	23 13 48.0	61 34 14	65	—
25	S 157	23 14 53.0	60 00 57	32	—
26		23 14 54.0	59 45 00	14	<9
27		23 15 32.1	59 36 22	34	—
28		23 15 50.5	59 36 07	12	—
29		23 15 55.7	59 52 13	14	—
30	S 162	23 17 11.0	60 44 02	15	—
31	S 157	23 17 25.2	59 41 31	21	—
32	S 162	23 17 37.6	61 13 03	56	—
33		23 18 01.3	60 47 19	19	—
34		23 19 25.3	61 01 13	11	—
35		23 21 18.1	60 44 08	120	—

This may be taken as an indication that S 156 lies in front or at the near edge of the neutral cloud complex discovered by Höglund and Gordon (1973). Short exposure photographs taken by Gull (Barlow et al., 1974) with the Kitt Peak 4 m telescope show extensive dust structure all around the edge of the bright central components of S 156. The blue Palomar Sky Survey print also shows a number of reflection nebulae in the vicinity of S 156.

2.2 Density Structure

A comparison of the λ 21 cm and λ 6 cm data gives no indication for the presence of optically thick components at λ 6 cm.

The λ 6 cm determination of the dimensions and flux-densities of the bright peak *A* implies an optical depth of 0.9 at λ 21 cm. For component A I find $n_e = 5\,10^3$ cm^{-2}. Glushkov and Karyagina (1972) and Deharveng (1974) both find a much higher electron-density from the [S II] lines at $\lambda\lambda$ 6717, 6731Å: $n_e = 1.9\,10^4$ cm^{-2}. This value is already near the limit where the [S II] lines yield useful results so that the actual density might be higher. From these data one derives that in the λ 6 cm radio map of component A the clumping factor f is 10 or higher. Thus component A is inhomogeneous, either in the sense that it consists of a number of small clumps or that a density gradient is present. A clumping factor of 10 also means that the actual mass of component A is only about 0.15 $M_\odot$. For the two smaller and less bright components, I find r.m.s. electron-densities of 3.1–3.4 10^3 cm^{-3}, while Deharveng (1974) finds an electron-density of 5–10 10^3 cm^{-3} from the [S II] lines, so that a clumping factor of 2.5–8.7 results. Therefore these two components show a similar inhomogeneity. At λ 6 cm I measure only 83 per cent of the envelope flux-density at λ 21 cm, somewhat less than expected on the basis of an optically thin thermal spectrum. The outer diameter of $90 \times 75''$ corresponds roughly to the size of the image on the red Palomar Sky Survey Print while the inner size of 35″ corresponds to the size of the bright part of the nebula. There are some indications for a density gradient in the envelope. The division in an outer and an inner envelope (Tables 4, 6) is somewhat artificial, and probably relates to a gradient. In fact, near-infrared observations by Persson and Frogel (1974) made with different diaphragm apertures ranging from 15 to 55″ seem to confirm this picture.

2.3 Extinction

The availability of radio, optical and infrared data enables one to derive the extinction across the nebula. The λ 21 cm flux-density $S_{1415} = 2.3$ f.u. together with the total Hβ flux of $1.3\,10^{-14}$ Wm^{-2} (O'Dell, 1973; Mathews, private communication) yields $A_V = 3\overset{m}{.}7$ as an average for the whole nebula. From the S(Hα)/S(Hβ) ratio, Barlow et al. (1974) find $E_{B-V} = 1\overset{m}{.}2$.

The exciting star has likewise $E_{B-V} = 1\overset{m}{.}2$ (Kostjakova et al., 1968; Chopinet et al., 1973). Thus for S 156, the ratio between total and selective extinction $R = A_V/E_{B-V}$ is 3.

The extinction is however not uniform over the nebula (Barlow et al., 1976; Sibille et al., 1975).

From a comparison of Hβ observations and the present λ 6 cm radio observations, Barlow et al. (1976) find visual extinction values for different parts of the nebula. The visual extinction of S156 appears to be reasonably well established. For the whole nebula $A_V = 3\overset{m}{.}6$, while peaks in the central bright part reach $A_V = 5\overset{m}{.}$.

2.4 The Nature of S156

It is rather difficult to explain the ringlike structure of S 156 in terms of a conventional Strömgren sphere. An attractive alternative explanation is offered by the quasistationary "blister type" model of the sort proposed

© European Southern Observatory • Provided by the NASA Astrophysics Data System

1977A&A....59...27I

Table 6. Derived physical parameters

Name (1)	Mean linear Diameter d (pc) (2)	R.m.s. electron Density n_e (cm^{-3}) (3)	Emission measure E.M. (10^6 pc^{-6}) (4)	Mass $M(M_\odot)$ (5)	Excitation parameter u (pc cm^{-2}) (6)
S 156 A	0.16	5200	4.2	0.4	27
B	0.09	3630	1.1	0.04	11
C	0.09	3395	0.95	0.04	11
Inner envelope	0.71	620	0.27	4.3	30
Outer envelope	1.7	195	0.07	18	33 Total 44
G 110.25+0.01 A	0.39	345	0.05	0.41	11
B	0.22	490	0.05	0.11	7
Envelope	1.42	52	0.004	3.0	11 Total 14
S 157 A	1.3	235	0.07	9.8	28
B	0.09	5880	2.9	0.06	15
C	0.18	885	0.14	0.10	10
D	0.12	1410	0.24	0.06	9 Total 31
G 111.2−0.8	4.4	20	0.002	33	19
G 111.4−0.7	6.5	14	0.001	73	21
G 111.5−0.6	5.0	18	0.002	43	19 Total 26
S 158 A 1	0.18	2395	1.0	0.29	19
A 2	0.24	2095	1.1	0.60	23
A 3	<0.09	>2685	>0.6	>0.01	10
A Envelope	1.1	520	0.3	13.5	41 Total A 45
B 1	0.18	1915	0.7	0.23	16
B 2	0.29	1695	0.8	0.83	24 Total B 26
G Total	0.13	10900	14.5	0.49	37
G 1[a]	0.06	94300	210	0.001	16
G 2[b]	0.13	12625	20	0.1	36
G 3	0.06	3980	1.0	0.02	9
Shell	3.0	320	0.31	180	84 Total 89
S 159 A	0.12	10000	12.3	0.35	33
S 162 A Total	1.3	295	0.11	3.5	33
A 1 (Cometary)	0.55	580	0.19	0.55	22
A 2 (Bubble)	1.05	340	0.12	2.1	29
B	0.18	765	0.11	0.03	9
C Total	1.75	145	0.04	4.6	29
C 1	0.5	330	0.05	0.22	13
C 2	0.60	210	0.03	0.27	12
C 3	0.50	250	0.03	0.16	11
C Envelope	1.75	125	0.03	4.0	26 Total 39

[a] Based on a turnover frequency of 5 GHz with $S=0.12$ f.u.

[b] Based on a turnover frequency of 2 GHz with $S=1.4$ f.u.

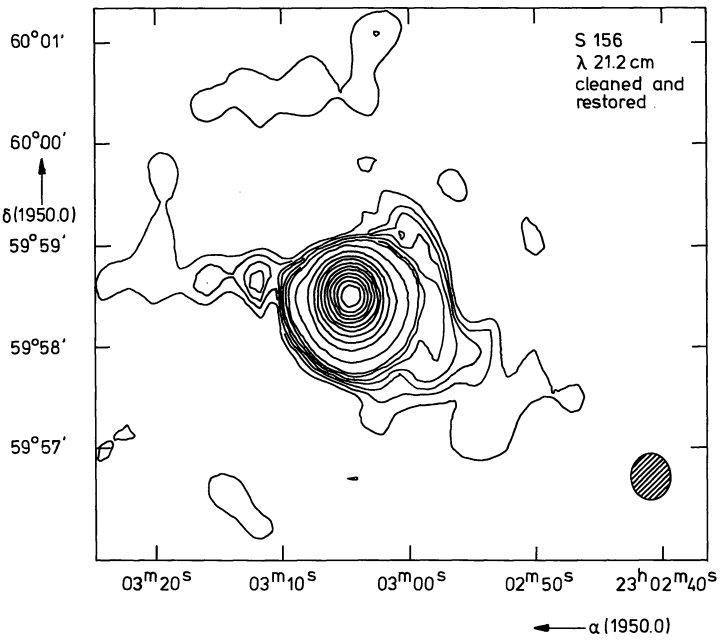

Fig. 1. S 156. Contour map at λ 21.2 cm, cleaned and restored. Contour values are 2.5, 5, 7.5, 10, 15, 20, 25, 50, 100, 150, 200, 250, 300, 350, 400, 450, 500 and 550 m.f.u. per synthesized beam area. The synthesized beam size is represented by a shaded ellipse in this and the following figures. Cleaned to a level of 5 m.f.u. per synthesized beam area

© European Southern Observatory • Provided by the NASA Astrophysics Data System

1977A&A....59...27I

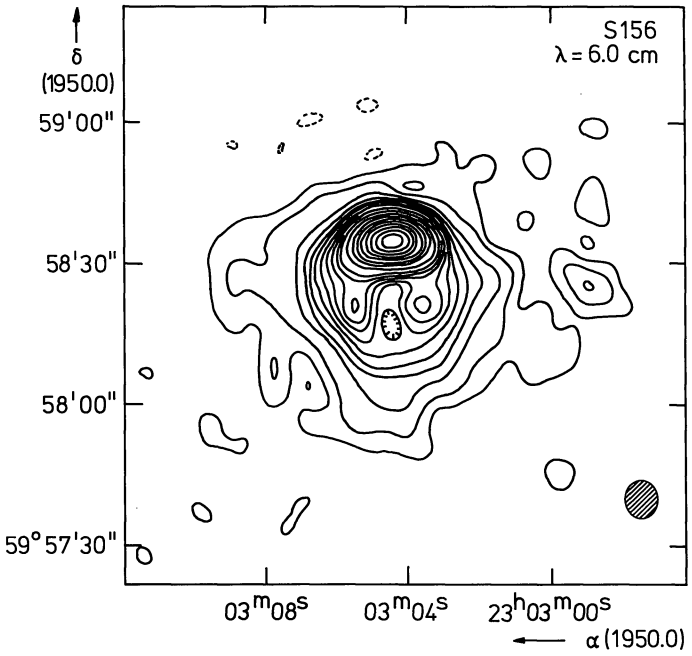

Fig. 2. S 156. Contour map at λ 6 cm. Contour values are 5, 10, 20, 30, 40, 50, 60, 70, 80, 90, 100, 125, 150, 175, 200, 225, 250, 275 and 300 m.f.u. per synthesized beam area. The dashed contour is −2.5 m.f.u. per synthesized beam area. Cleaned to a level of 2.5 m.f.u. per synthesized beam area

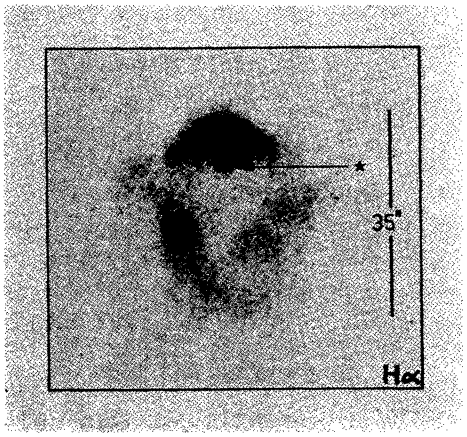

Fig. 3. S 156. Photograph in Hα light by L. Deharveng. The position of the exciting star is indicated. Due to the short exposure, only the bright core components of S 156 are visible. Note the good correspondence between this figure and Figure 2

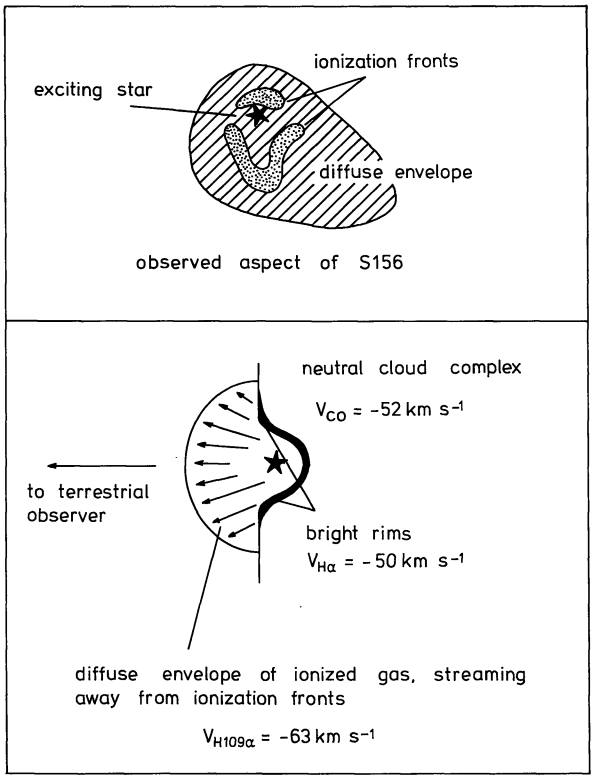

Fig. 4. Schematic representation of S 156. Top: view from Earth. Bottom: proposed view at right angle to line of sight

for Orion A (Zuckermann, 1973; Balick et al., 1974), Orion B (=NGC 2024; Grasdalen, 1974) and S 206 (=NGC 1491; Deharveng et al., 1976). In that case the following situation applies (see Fig. 4).

i) The exciting star is located at the edge of the neutral cloud complex found by Höglund and Gordon (1973).

ii) The star ionizes the nearby parts of the neutral cloud. The resulting ionization fronts are visible as core components of S 156 (large clumping factor).

iii) Ionized gas is streaming away from the ionization fronts and forms the envelope component (small clumping factor).

This simple model explains or is consistent with a number of observations. On the basis of its velocity, S 156 is associated with the neutral cloud complex, yet the object is well visible and does not suffer overly from extinction. The ring components look very much like bright rims; their degree of excitation is low ([O III]/Hβ = 2.8) and the ratio of [N II] to Hα is low (Deharveng, 1974). The exciting star is of type O7 (Glushkov and Karyagina, 1972); such a star has an excitation param-

© European Southern Observatory • Provided by the NASA Astrophysics Data System

1977A&A....59...27I

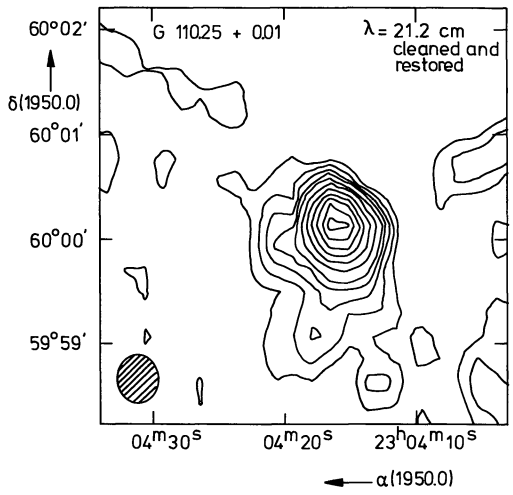

Fig. 5. G 110.25+0.01. Cleaned and restored contour map at λ 21 cm. Contour values are 1.5, 3, 4.5, 6, 7.5, 10, 12.5, 15, 17.5, 20 and 22.5 m.f.u. per synthesized beam area. Cleaned to a level of 5 m.f.u. per synthesized beam area

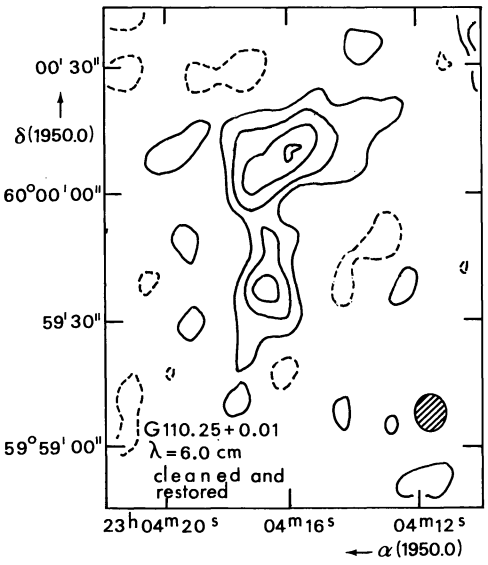

Fig. 6. G 110.25. Cleaned and restored contour map at λ 6 cm. Contour values are 1.5, 3, 4.5 and 6 m.f.u. per synthesized beam area. The dashed contour is −1.5 m.f.u. per synthesized beam area. Cleaned to a level of 1 m.f.u. per synthesized beam area

eter of at least 52 pc cm^{-2} (Panagia, 1973), while only 41 pc cm^{-2} is observed in the radio regime. Thus only about half the number of Lyman continuum photons emitted by the star are taken up by the gas of S 156 (cf. also Barlow et al., 1976). Finally it should be noted that S 156 is not the only object on the outer edge of the neutral cloud complex: at least three stars bright enough to give rise to reflection nebulae, but not bright and hot enough to ionize an appreciable amount of neutral matter ($S_{4995} < 10$ m.f.u.) are also located within the boundaries of the cloud.

3. G 110.25+0.01

In paper I we discussed an anonymous H II region near S 156. A cleaned map at λ 21 cm is given in Figure 5. This region was reobserved at λ 6 cm, although not during a full twelve hour period (see Table 4). The resulting map was cleaned and restored (Fig. 6).

The λ 6 cm flux-density quoted in Table 4 has a fairly large error because the object was some 5′ away from the observed field center, resulting in a weakening by a factor 2.3 due to the decrease in the primary beam sensitivity G 110.25+0.01 appears to consist of two components with flux densities of about 40 and 15 m.f.u. respectively and sizes of 19″ and 11″ respectively. The object coincides with a secondary peak in the CO distribution of the neutral cloud complex associated with S 156 (Blair, private communication). Since it is optically visible it also must be on the near side of the cloud complex. Its distance will therefore indeed be the same as that of S 156, so that I take $D = 3.5$ kpc. The object is partially obscured. It shows a core-envelope structure at λ 21 cm.

4. S 157

4.1. Extended Components

Using the clean procedure, I removed the disturbing influence of S 157A and B on their surrounding in the λ 21 cm map. The cleaned map (Fig. 7) shows the presence of two extended components, the easternmost having a complex structure. No connection between the two extended components and the compact objects S 157A and B is visible. The total radio emission detected ($S_{1415} = 2.5$ f.u.) is still only a fraction of the total flux density of S 157 ($S_{1415} = 20-40$ f.u., cf. Paper I). The two extended regions are rather tenuous with r.m.s. electron densities of the order of 15–20 cm^{-3}. The low excitation parameters indicate excitation by a late O star or early B stars.

Both objects have optical counterparts (Fig. 8). G 111.4−0.6 is partially obscured by dust bands. G 111.2 −0.8 is almost at half power; its structure is therefore somewhat uncertain (the more so because of the distorting influence of weak grating rings due to Cas A at a distance of 1.5 degree, indicated in Figure 8). The radio maxima appear coincident with optical brightness peaks. At the eastern edge of G 111.2−0.8 a weak obscured point source (#20) is visible with $S_{1415} = 25$ m.f.u. Its nature is uncertain. If it is an H II region, it should have $n_e \geqq 375$ cm^{-3}, E.M. $\geqq 4\ 10^4$ pc cm^{-6} and $u = 9$ pc cm^{-2}. It might be a compact H II region.

4.2. Compact Component

The bright H II knot in S 157 was optically studied by Chopinet and Lortet-Zuckermann (1972) and by Deharveng (1973, 1974). Near-infrared observations

© European Southern Observatory • Provided by the NASA Astrophysics Data System

1977A&A....59...27I

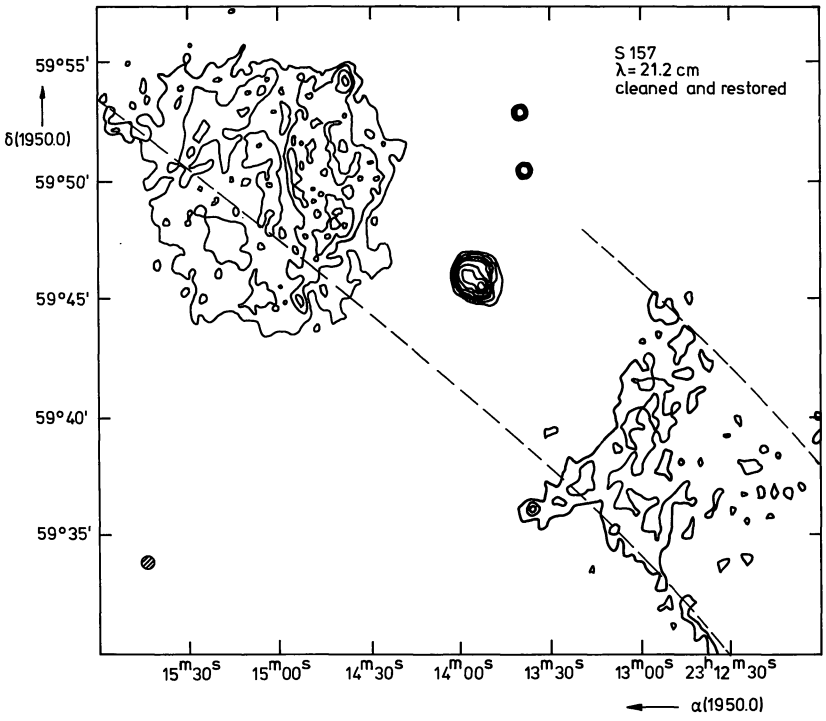

Fig. 7. S 157. Cleaned and restored contour map at λ 21 cm. Contour values are 5, 10, 15, 20, 25, 50, 75 and 100 m.f.u. per synthesized beam area. The compact object in the center is S 157 A and B. The extended object to the left is G 111.4 − 0.6 and the one to the right is G 111.2 − 0.8. Two grating responses due to the nearby supernova remnant Cas A are indicated by dashed lines. Cleaned to a level of 7.5 m.f.u. per synthesized beam area

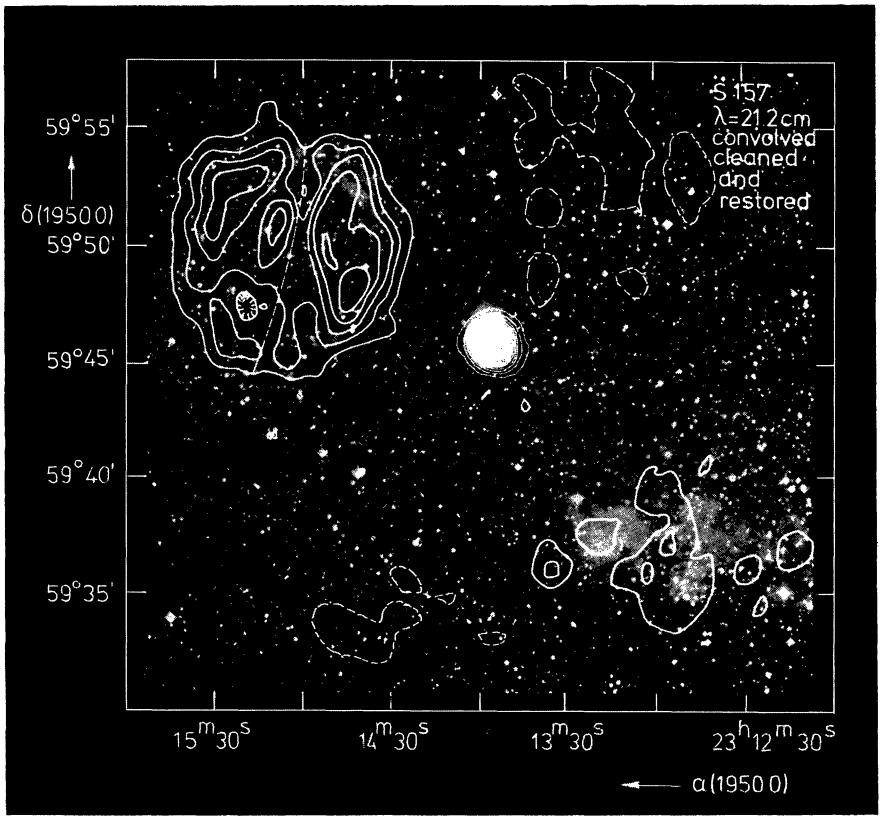

Fig. 8. S 157. Contour map at λ 21 cm overlaid on red Palomar Sky Survey print. The map is convolved to a 1′ beam. Contour values range from 20 to 400 m.f.u. per synthesized beam area in intervals of 20 m.f.u. per synthesized beam area. The dashed contour is −20 m.f.u. per synthesized beam area. Sources #21 and #22 are subtracted

were obtained by Lunel et al. (1974). A comparison of the λ 6 cm map and an isodensitogram in Hβ shows that optically only the eastern half of the knot (called S 157A) is observed. The western half contains a very bright compact radio source (S 157B) with an angular diameter of 4″ (corresponding to a cylindrical linear diameter of 0.09 pc). Two other compact components C and D in Paper I, which are now called sources #21 and #22 in Table 6. A further discussion of S 157 A and B will be presented in a later paper.

© European Southern Observatory • Provided by the NASA Astrophysics Data System

1977A&A....59...27I

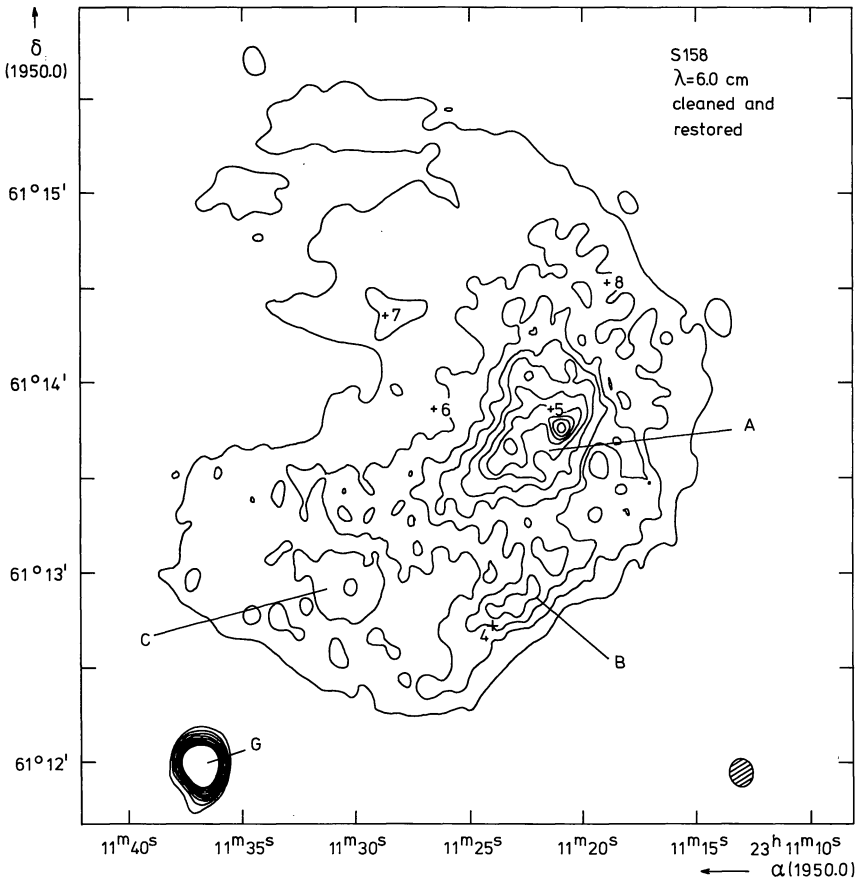

Fig. 9. S 158. Contour map at λ 6 cm. The map is cleaned and restored. Contour values are 20 to 200 m.f.u. per synthesized beam area, with intervals of 20 m.f.u. per synthesized beam area. The positions of infrared sources found by Wynn-Williams et al. (1974) are indicated by crosses. Cleaned to a level of 17.5 m.f.u. per synthesized beam area

5. S 158 (NGC 7538)

5.1. Optical Aspects

S 158 has the form of an incomplete, open shell. A bright ridge with a complex structure, or perhaps a series of ridges characterizes the southwestern half of the nebula. The ridges contain bright spots. The eastern half on the nebula is less bright and more diffuse. Short exposure optical photographs taken under good seeing conditions show structures in the northeastern part that look like elephant trunks and bright rims. Indeed, according to Glushkov et al. (1975) component F of Paper I is a bright rim structure with an electron density of 2900 cm^{-3} and an extinction $A_V = 6^m.5$. On the red Palomar Sky Survey print the southern edge appears to be limited by the foreground dust. Thus the nebula is photon limited at least partially.

An O 7 star is located in a brightness minimum about 25″ east of the brightest western ridge (component A). This star is responsible for at least part of the excitation of S 158. This star has $A_V \approx 5^m$ (Chopinet et al., 1973; Glushkov et al., 1975). Gebel's (1968) Hα intensity yields together with $S_{1415} = 22$ f.u. (Paper I) an extinction $A_V = 4^m.6$.

The extinction of S 158 is well established with $A_V = 4^m.5 \pm 0^m.5$ and seems to vary little over the brightest parts of the nebula.

In ridge *A*, a second early type star (possibly O 5 or O 6; Glushkov and Karyagina, 1972) is located very close to the brightest part of S 158. This star is more obscured than the nebula with $A_V \geqq 8^m$ (Glushkov et al., 1975). The compact source G is completely obscured except for possibly component G 2 that coincides with a faint optical wisp.

5.2. Radio Aspects

The radio map at λ 6 cm (Fig. 9), resembles the optical picture closely, except for the presence of the compact source *G*. Within an area 3.6′ across, a flux density $S_{4995} = 20$ f.u. is observed, yielding an r.m.s. electron density of 270 cm^{-3} and an emission measure of $3\,10^5$ cm^{-3} for S 158 as a whole. Since the brightness distribution in both the optical and the radio is very uneven, local r.m.s. electron densities may be higher. For different bright parts of S 158, Glushkov and Karyagina (1972) find electron densities from the [S II] doublet of the order of 1500 cm^{-3}. Thus the clumping factor f is of the order of 17. The lower limit to the mass of S 158 is then 43 $M_\odot$, while the upper limit is 180 $M_\odot$ (Table 6).

5.3. S 158A and B

At λ 6 cm, component A contains about 2.7 f.u. The small-scale structures in A depicted in Figure 10 (see also

© European Southern Observatory • Provided by the NASA Astrophysics Data System

1977A&A....59...27I

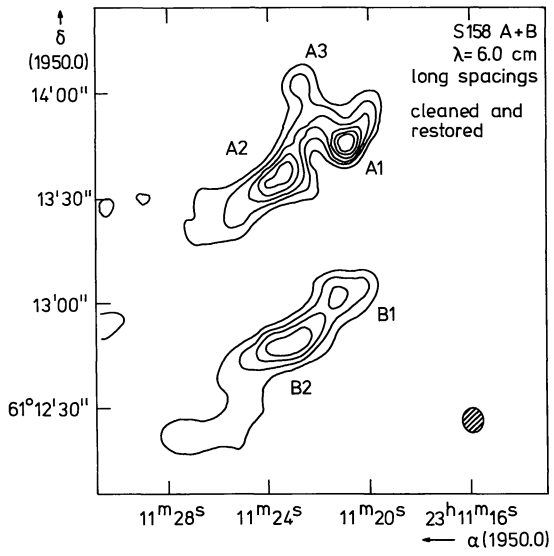

Fig. 10. S 158 A and B. Cleaned and restored contour map at λ 6 cm, containing only the long spacings. Contour values are 10, 20, 30, 40, 50 and 60 m.f.u. per synthesized beam area

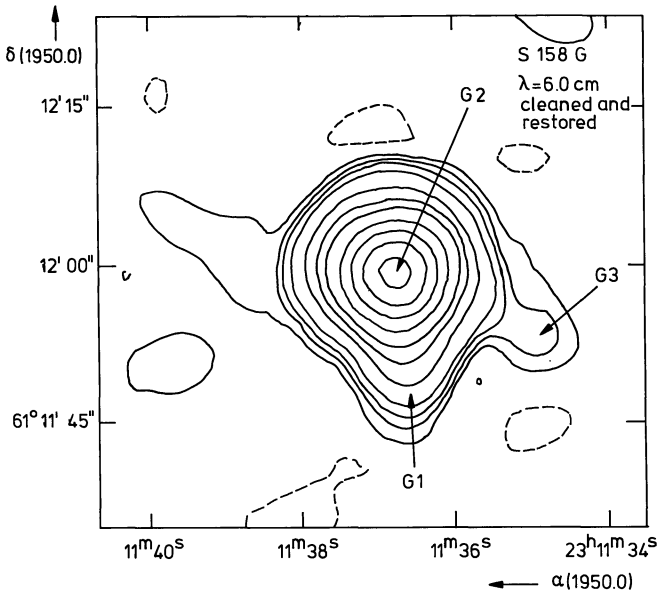

Fig. 11. S 158 G. Contour map at λ 6 cm. The map is cleaned and restored and contains only long spacing information. Contour values are 10, 20, 30, 50, 100, 150, 200, 300, 400, 500 and 600 m.f.u. per synthesized beam area. Dashed contour is −10 m.f.u. per synthesized beam area

Sect. II) represent only 0.6 f.u. Component A has a definite ridge structure. Infrared source S 158-IRS5 (Wynn-Williams et al., 1974a) coincides with the bright maximum S 158 A1. This maximum includes a condensation that might be a compact H II region. It is unresolved ($\theta_G < 4''$ or $d \leqq 0.08$ pc) with a flux density $S_{4995} = 160$ m.f.u. Its r.m.s. electron density must therefore be higher than $7.3\,10^3$ cm^{-3}, its emission measure is at least $4.4\,10^6$ pc cm^{-2}. Since its excitation parameter is only 18 pc cm^{-2}, it is impossible to determine whether this compact object is excited internally, from the outside by the nearby early O star. I consider most of the emission from A1, A2 and A3 as coming from an ionization front and an associated envelope component. The high extinction O star is probably the exciting star for component A.

Glushkov and Karyagina (1972) find a peak density of 9350 cm^{-3} in ridge *A*, so that a maximum clumping factor $f = 56$ is indicated.

A second, weaker ridge is visible in both the optical and the radio somewhat south of S 158 A (Fig. 11). This ridge *B* contains about 0.5 f.u. at λ 6 cm. It has two brightness peaks, and coincides with near infrared source S 158-IRS 4 (Wynn-Williams et al., 1974a). R.m.s. electron densities in ridge *B* are of the order of a few times 10^3 cm^{-3}. Ridge *B* is probably also an ionization front. It is not clear whether it is ionized by the clearly visible O 7 star, or by the later discovered high extinction O star.

5.4. S 158 G

By far the most interesting object in S 158 is the compact component *G* (Habing et al., 1972; Paper I). It was mapped with 2″ resolution at λ 6 cm by Martin (1973) who found three separate components. He resolved one of these (which I call *G2*) clearly: it has the form of an incomplete ring. A second component (here called G1) is just resolved and coincides with an OH maser (Wynn-Williams et al., 1974b). Wink et al. (1975) confirm these results at λ 3.7 cm. Figure 11 shows the WSRT map of source G (long spacings only), while the spectrum of both source G as a whole and that of component G1 are shown in Figure 12. On the basis of the turnover frequency of 5 GHz for G1, I determined a diameter of 0.7″ (corresponding to 12000 A.U. at a distance of 3.5 kpc). The derived angular diameter of about 1″ is confirmed by Lo (1974) at λ 3.7 cm; it is less than the value found by Martin (1973) who gives 1.2″ × 2.0″. The high electron density of 10^5 cm^{-3} and the high emission measure of $2\,10^8$ pc cm^{-2} make S 158 G1 comparable to W58 A1 (Israel, 1976 here after called Paper II), the compact source close to K3–50. If the turnover frequency is not 5 GHz, but 7 GHz as suggested by Lo's (1974) observation, the parameters of G 1 will be even more extreme.

Downes and Wilson (1974) presented convincing evidence for the presence of a dense neutral shell surrounding S 158 G1.

5.5. The Nature of S 158

S 158 is associated with a dense molecular cloud (Table 7). Wilson et al. (1974) observed CO emission at various positions near S 158, while the whole area was mapped by Dickel et al. (private communication). The CO emission peaks a few arc min south of S 158, with $V_{LSR} = -57$ km s^{-1}. The other detected molecules have the same radial

© European Southern Observatory • Provided by the NASA Astrophysics Data System

1977A&A....59...27I

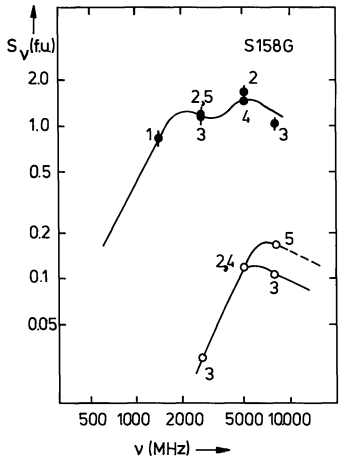

Fig. 12. Spectrum of compact source G. Filled circles indicate flux densities of all components of G, open circles refer to compact component G 1. Paper I, 2. This paper, 3. Wink et al. (1975). 4. Martin (1973). 5. Lo (1974)

velocity. Minn and Greenberg (1975) detected H_2CO clouds in absorption, one of which appears to be associated with S 158, with $V_{LSR} = -55.5$ km s^{-1}.

The molecular velocities are somewhat less negative than the ionized hydrogen velocities ($V_{LSR} = -60$ km s^{-1}, cf. Table 2). Thus the ionized gas appears to be streaming away from the associated neutral cloud with a velocity of about -3 km s^{-1} in the line of sight. Such a velocity difference might be characteristic of a situation similar to the model proposed in Section III. 2.4 for S 156. In effect, Zuckerman (1973) already mentioned S 158 as a possible candidate for such a model.

Both the morphology of S 158 and the observed small blueshift of S 158 with respect to the neutral cloud suggest that the process is seen almost edge-on (viewing angle about 70°) as in the cases S 206 (=NGC 1491; Deharveng et al., 1976) and M 17 (Meaburn; 1975). Unlike NGC 1491, S 158 appears to be the seat of active star formation processes, although on a more modest scale than in M 17.

Star formation is possibly going on in or near ridge A; it is certainly going on in source G. It is remarkable that source G is located south of S 158, in the direction of the neutral maximum. This orientation holds even inside source G itself: the halfring G 2 is brightest in the south (it might be an ionization front itself), and the observed compact component G 1 is again south of G 2. Farther south a second OH maser is found (the first being associated with G 1) that has no known radio emission ($S_{4995} < 5$ m.f.u.) or infrared emission. Presumably it is located at a place of even higher density. As in the case of W 58 (Paper II), it appears that star formation started on the outside of a neutral cloud and is now moving inwards, thereby gaining in intensity.

A critical test of the rough model suggested here lies in detailed observations of the velocity field of S 158. To date, the only available data are H94α observations by

Table 7. Molecules near S 158

Species	Velocity V_{LSR} (km s^{-1})	Column density N (cm^{-2})	Reference
(1)	(2)	(3)	(4)
CO	−57	$1\,10^{19}$	Wilson et al. (1974)
CN	−57.4	$1\,10^{14}$	Turner and Gammon (1975)
CS	−56.5	—	Turner et al. (1973)
CH	−56	$7\,10^{13}$	Rydbeck et al. (1975)
HCN	−57.7	—	Morris et al. (1974)
C_2H	−56.8	—	Tucker et al. (1974)
H_2S	−57.2	$4\,10^{13}$	Thaddeus et al. (1972)
H_2CO	−59	$>2\,10^{14}$	Downes and Wilson (1974)

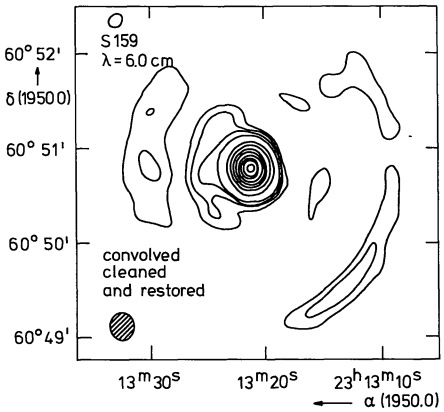

Fig. 13. S 159. Cleaned and restored contour map at λ 6 cm, convolved to a beam of 16″.5. Contour values are 10, 20, 30, 50, 100, 150, 200, 250, 300, 350, 400 and 450 m.f.u. per synthesized beam area. The structure of the weak, extended component is severely distorted by imperfect sidelobe structure due to the compact component S 159 A. Cleaned to a level of 5 m.f.u. per synthesized beam area

Lada and Chaisson (1973). They find a velocity gradient from -61 to -58 km s^{-1} in an eastern direction which is what one would expect from projection effects only. Their resolution both in space and velocity was poor (4′2 and 6.4 km s^{-1} respectively), so that these results are not conclusive. Lada and Chaisson themselves attributed the gradient to rotation. This is unlikely, because of the apparent association of S 158 with a large neutral cloud.

6. S 159

6.1. S 159A

Between S 158 and S 162 a diffuse emission region with an optically very bright wisp is visible. At the position of the wisp, a pointlike source was observed in the λ 21 cm fields of both S 158 and S 162, with a flux density $S_{1415} = 0.8 \pm 0.2$ f.u. This source appeared to have a diameter of 12″ (Paper I). The new λ 6 cm observations (Fig. 13) show the pointlike source to be resolved with a (gaussian) diameter of about 6″ corresponding to a linear diameter of 0.12 pc at a distance of 3.5 kpc. Thus the λ 21 cm

© European Southern Observatory • Provided by the NASA Astrophysics Data System

1977A&A....59...27I

diameter appears to have been overestimated. The λ 6 cm emission measure shows that the source spectrum should turn over at a frequency of 1.6 GHz. The source is thus optically thick at λ 21 cm ($\tau_{1415} = 1.9$).

It is useful to note that the λ 6 cm radio observation does not differentiate between one resolved component or two close, unresolved components. The geometry of S 159A might thus be similar to that of W 58A (the K3-50 source) discussed in Paper II. In that case it would be a very young object. It is also worthwhile to note that S 159 is near a peak of CO emission in the same complex that is associated with S 158 (Dickel, private communication). The CO velocity in the direction of S 159A is $V_{LSR} = -56$ km s^{-1}. The cloud near S 159 has a size of 6 pc (Israel, unpublished). Unfortunately, the radial velocity of S 159A is not known. Recently, also CH emission was discovered in the same direction (Hjalmarson et al., 1975), and with the same velocity as the CO.

6.2. S 159B

On the red Palomar Sky Survey print one finds a diffuse region with a size of 3'5 directly east of S 159A. Traces of this region are visible in both the λ 21 cm and λ 6 cm (Fig. 13) radiomaps.

However, at λ 21 cm the source is too far from the field center and disappears into the noise, while at λ 6 cm the dynamic range of the telescope is not sufficient to see a region with such a low surface brightness near S 159A.

Terzian et al. (1973) observed S 159 (their source Anon I) with a single dish telescope. They found $S_{2695} = 2.6$ f.u. From the WSRT observations one knows that S 159A contributes about 1 f.u., so that S 159B flux density of 1.5 f.u. at 6 cm. From this and the optical size I derive the following properties: linear size 3.6 pc, r.m.s. electron density $n_e = 74$ cm^{-3}, emission measure E.M. $= 2\,10^4$ pc cm^{-2}, mass $M = 71\ M_\odot$ and excitation parameter $u = 37$ pc cm^{-2}.

The morphology of S 159 and the association with a neutral cloud open the possibility that the same model proposed for S 156 and S 158 also applies to S 159.

7. S 162 + NGC 7635

7.1. Optical Aspects

The relatively large ($\theta_G \approx 60'$) diffuse nebula S 162, containing the bubble-like NGC 7635 has attracted considerable interest in the past. Its nature was discussed extensively by Johnson (1971) and in Paper I. Optical studies were published by Doroshenko (1972), Deharveng (1973), Johnson (1974a) and Barlow et al. (1974). Date on the exciting star were given by Doroshenko (1972) and Viotti and Nesci (1974). In Paper I we published high resolution radio observations at λ 21 cm. From these observations, the following picture has now emerged.

S 162 is a well evolved H II region of relatively low density, containing many bright rims. The nebula is excited by the O6.5IIIf star BD + 60°2522. This star is also the exciting star of the Bubble nebula NGC 7635. The Bubble nebula is probably due to mass loss of the exciting star; the expanding gas clouds collide with the surrounding nebular gas which has an inhomogeneous density distribution. The very regular morphology of the Bubble nebula can be explained in this way (Icke, 1973). Of particular interest is a cometary nebula inside the Bubble, near the exciting star (component A1 in Paper I). This cometary nebula was studied by Deharveng (1973) and Johnson (1974). It is not an internally excited compact H II region, but it shows clear characteristics of a complicated bright rim structure (Barlow et al., 1974, 1976).

7.2. The Bubble Nebula

The new λ 6 cm radiomap (Fig. 14) contains a wealth of detail[2]. The radio structure resembles the optical structure; most of it is still partially unresolved, indicating clumping factors appreciably larger than unity. In Tables 4 and 6 only the overall parameters are given. Note that the λ 21 cm flux-densities for A1 and A2 differ strongly from the values given in Paper I. The reason for this is that the information on the structure, given in the λ 6 cm map enables one to make a much better separation between the two components than at λ 21 cm. The sum of the flux densities was of course not affected by this revision.

The r.m.s. electron density of the bright northern part of the Bubble nebula (component A2) derived from the λ 6 cm radio observations is 370 cm^{-3}, in good agreement with the values of 370 and 545 cm^{-3} derived from the Hα surface brightness by Doroshenko (1972). Deharveng (1973) shows that the actual densities as derived from the [S II] lines of this part of the Bubble nebula may be as high as 2500—5000 cm^{-3}, while Glushkov (private communication) finds an electron-density of 6300 cm^{-3} for a position in the shell, but only 1500 cm^{-3} for another position (Glushkov, 1972).

For the different individual features in the shell I derive r.m.s. electron densities of 2500—3200 cm^{-3}, confirming mean sizes of the order of 1–2" ($d \approx 0.03$ pc). The radio surface brightness is about $2\,10^{-30}$ W m^{-2} Hz^{-1} arcsec^{-2} for these bright filaments. Their emission measure is around $2\,10^6$ pc cm^{-2}. These parameters are consistent with the model derived by Icke (1973).

7.3. The Cometary Nebula

There can be little doubt about the physical association of the different objects seen within the boundaries of S 162 (cf. Barlow et al., 1974). For the cometary structure (component A1) as a whole I find an r.m.s. electron density $n_e = 1100$ cm^{-3}.

[2] Somewhat too much actually. Instrumental imperfections introduced an artificial ridge, indicated by a dotted line in Figure 11

© European Southern Observatory • Provided by the NASA Astrophysics Data System

1977A&A....59...27I

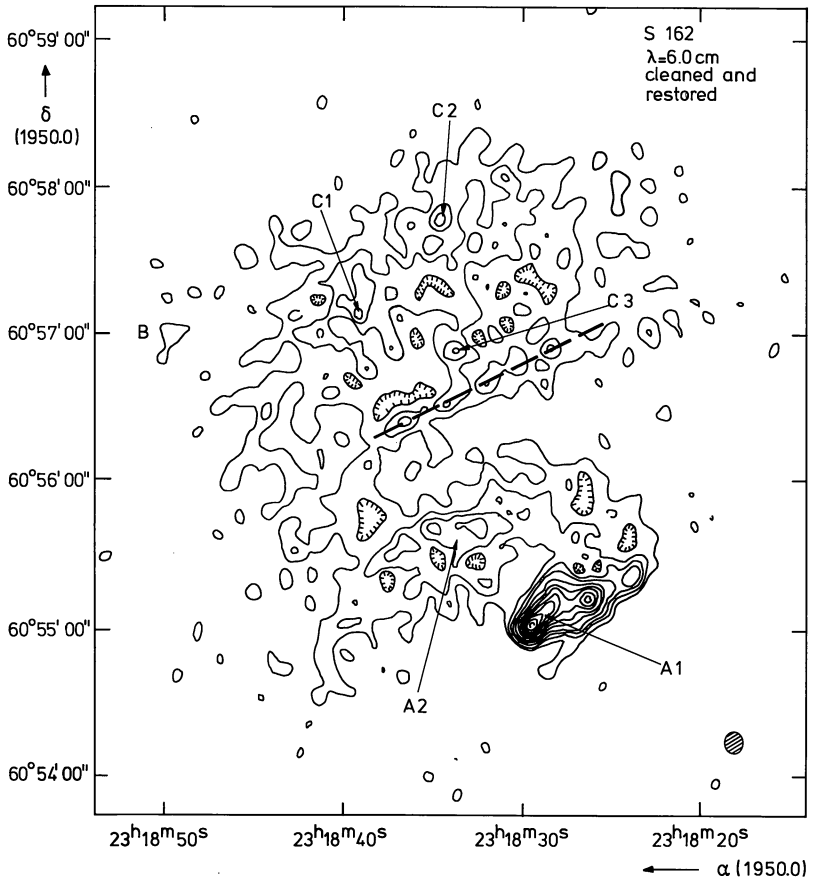

Fig. 14. S 162. Contour map at λ 6 cm. Contour values are 2.5, 5, 7.5, 10, 15, 20, 25, 30, 35, 40, 45, 50, 55, 60, 65, 70, 75, 80, 85, 90, 95, and 100 m.f.u. per synthesized beam area. An artificial bar, due to instrumental imperfections is indicated by a dashed line. Cleaned to a level of 5 m.f.u. per synthesized beam area

On the basis of physical properties derived from the radio map and electron densities found by Deharveng (1973) and Glushkov (1972), I conclude that the cometary nebula contains knots on a typical linear scale of 0.05–0.1 pc and with typical densities of $3\,10^3$ to $1.2\,10^4$ cm^{-3}. With such densities, some knots may be optically thick at λ 21 cm.

7.4. The Bright Rim Complex

North of the Bubble nebula, a very complicated bright rim structure is seen, called sources C and B in Paper I. Likewise, the λ 21 cm flux densities quoted in Paper I are revised in Table 4. Moreover, in the original λ 21 cm map the flux density of *B* was overestimated by a factor of two. In Paper I we already warned that the structure of bright rim complex C was more complicated than assumed in the derivation of physical parameters. For the complex C as a whole, I find $S_{4995} = 665 \pm 200$ m.f.u. The main uncertainty in the flux density is caused by the determination of the local zero level: it is not clear exactly what part of the emission originates in source C and what part is due to the overall diffuse emission of S 162. Individual peaks in the complex have flux densities of the order of 10–20 m.f.u. and radio sizes between 3″ and 8″, thus yielding r.m.s. electron densities in the range of 600–4000 cm^{-3}. For the diffuse component surrounding these peaks, an r.m.s. electron density of about 200 cm^{-3} is found. Glushkov (private communication) determined densities from the [S II] lines for complex C. In the bright peaks, he found densities around 5500 cm^{-3}, for less bright parts densities ranging from 1500–4000 cm^{-3}. The agreement is reasonable and again indicates typical linear scales of 0.05–0.1 pc for radiating structure in the rim area. One notes finally, that the diffuse emission between complex *C* and the Bubble comes from a region with an r.m.s. electron density of 120 cm^{-3}, which is considerable more than the average value of 46 cm^{-3} for all of S 162 (Paper I). Clearly, a density gradient is present in S 162.

IV. Conclusions

In Paper I we suggested that the regions around 1 = 111° form a loose OB association in a very early stage of its evolution. We assumed that each H II region was representative of a stellar subgroup in this association. The present study appears to confirm this picture. At least two neutral cloud groups are present in the area; one is associated with S 156 and G 110.25 + 0.01, the other with S 158 and S 159. Both have typical sizes of 25 pc.

The S 156 cloud contains two H II regions and three reflection nebula. All five coincide with neutral maxima. Thus, the S 156 group consists of at least two O stars and three B stars. The S 158/S 159 subgroup contains at least six O stars. Most of these can be found in a 5 pc wide

© European Southern Observatory • Provided by the NASA Astrophysics Data System

1977A&A....59...27I

region near S 158: in S 158 two O stars are visible, and two or three are hidden in source G. One O star appears to be forming at the position of the southern OH maser.

Neutral clouds are also present near S 157. It is difficult to interpret the very complex region S 157 properly, but the observations show that again at least three O stars and one B star must be present in addition to the Wolf Rayet star HD 219460. S 162 does not contain compact H II regions indicative of active star formation. The region appears to be in a late evolutionary stage (cf. Paper I). Significantly, no CO emission is detected near S 162 (Wilson et al., 1974; Dickinson et al., 1975); neither is HCN or CS (Morris et al., 1974). In S 162, one O 6.5 star with strong mass loss is known, but others of later type may well be present in the region.

In Paper II, I found evidence that in W 58 star formation occured first at the edge of the cloud complex, and subsequently moved inwards, at the same time becoming more intense. The present study gives a symilar impression for the H II regions around $1 = 111°$.

As mentioned before, the S 156 neutral complex shows five nebulae (of which three are reflection nebulae) associated with maxima in the CO distribution. No radio sources are found at the position of two other maxima. Thus the majority of young stars associated with this complex are on the near side of the neutral cloud; the good visibility of their surrounding nebulae indicates that they are also near the outer edge of the cloud.

The same behaviour is shown even more clearly by S 158 (cf. Sect. III-5.5). Here again the H II region that appears most evolved is farthest from the nearest CO maximum, while less evolved features like source G and the southern OH source are located closer to that maximum. Moreover, source G seems to contain half the exciting stars of S 158 in a region less than 0.2 pc across.

At least two regions out of six (S 156 and S 158) have a structure similar to the proposed for the Orion nebula by Zuckermann (1973) and Balick et al. (1974). This model proposes that an early type star creates a cavity in the associated neutral cloud, from which ionized gas streams away. Characteristic of such regions appear to be broad, curved ridges, that give the impression of an incomplete shell: very bright on one side, much weaker on the other. Both S 156 and S 158 show such a form. It is interesting to note that also G 110.25+0.01 and, on a much smaller scale, S 158G2 show a similar structure. In this respect, it is also interesting to see whether S 157B and S 159A have this kind of structure.

S 162 gives a different appearance. However, this might be largely due to the late evolutionary stage in which the region finds itself. There are some indications that S 162 also has the form of a cavity in the surrounding dust cloud.

Based on this limited, but complete sample of H II regions in the Perseus Arm, one might suspect (as did Zuckermann, 1973) that H II regions of the proposed semi stationary type are very common.

Thus, the following conclusions can be drawn:

(i) Formation of OB stars occurs in groups.

(ii) Stars form at the edges of neutral clouds.

(iii) A majority of H II regions may be in a semi stationary state.

References

Baars, J. W. M., Hooghoudt, B. G.: 1974, *Astron. Astrophys.* **31**, 323

Balick, B., Gammon, R. H., Hjellming, R. M.: 1974, H II Regions and the Galactic Center, 8th ESLAB Symposium, Ed. A. F. M. Moorwood ESRO SP 105, p. 135

Barlow, M. J., Cohen, M., Gull, T. R.: 1974, H II Regions and the Galactic Center, 8th ESLAB Symposiom, Ed. A. F. M. Moorwood, ESRO SP 105, p. 23

Barlow, M. J., Cohen, M., Gull, T. R.: 1976, *Monthly Notices Roy. Astron. Soc.* **176**, 359

Blair, G. N., Peters, W. L., Vanden Bout, P. A.: 1975, *Astrophys. J. Letters* **200**, L 161

Casse, J. L., Muller, C. A.: 1974, *Astron. Astrophys.* **31**, 333

Cato, B. T., Rönnäng, B. O., Lewin, P. T., Rydbeck, O. E. H., Yngvesson, K. S., Cardiasmenos, A. G., Shanley, J. F.: 1975, Research Report no. 123, Chalmers University, Gothenburg (Sweden)

Chopinet, M., Lortet-Zuckermann, M. C.: 1972, *Astron. Astrophys.* **18**, 373

Chopinet, M., Georgelin, Y. M., Lortet-Zuckermann, M. C.: 1973, *Astron. Astrophys.* **29**, 225

Deharveng, L.: 1973, 18e Colloque International d'Astrophysique, Liége, p. 357

Deharveng, L.: 1974, *Astron. Astrophys.* **35**, 63

Deharveng, L., Israel, F. P., Maucherat, M.: 1976, *Astron. Astrophys.* **48**, 63

Dickinson, D. F., Frogel, J. A., Persson, S. E.: 1974, *Astrophys. J.* **192**, 347

Doroshenko, V. M.: 1972, *Astron. Cirk.* no. 609

Downes, D., Wilson, T. L.: 1974, *Astrophys. J. Letters* **191**, L 77

Fanti, C., Felli, M., Ficarra, F., Salter, C. J., Tofani, G., Tomasi, P.: 1974, *Astron. Astrophys. Suppl.* **16**, 43

Gebel, W. L.: 1968, *Astrophys. J.* **153**, 743

Georgelin, Y. M.: 1975, thesis Univ. de Provence, Obs. de Marseille (France)

Glushkov, Yu. I., Karyagina, Z. V.: 1972, *Astron. Cirk.* no. 711

Glushkov, Yu. I., Denisyuk, E. K., Karyagina, Z. V.: 1974, *Astron. Astrophys.* **39**, 481

Grasdalen, G. L.: 1974, *Astrophys. J.* **193**, 373

Habing, H. J., Israel, F. P., Jong, T. de: 1972, *Astron. Astrophys.* **17**, 329

Harten, R. H.: 1976, *Astron. Astrophys.* in preparation

Hjalmarson, A., Sume, A., Elldér, J., Rydbeck, O. E. H., Moore, E., Huguenin, R., Sandquist, A. A., Lindblad, P. O., Lindroos, P. O.: 1975, Research Report no. 124, Chalmers University, Gothenburg (Sweden)

Högbom, J.: 1974, *Astron. Astrophys. Suppl.* **15**, 417

Högbom, J., Brouw, W. N.: 1974, *Astron. Astrophys.* **33**, 289

Höglund, B., Gordon, M. A.: 1973, *Astrophys. J.* **182**, 45

Icke, V.: 1973, *Astron. Astrophys.* **26**, 45

Israel, F. P.: 1976, *Astron. Astrophys.* **48**, 193

Israel, F. P., Habing, H. J., Jong, T. de: 1973, *Astron. Astrophys.* **27**, 143

Jenkins, E. B., Savage, B. D.: 1974, *Astrophys. J.* **187**, 213

Johnson, H. M.: 1971, *Astrophys. J.* **167**, 491

Johnson, H. M.: 1974a, *Astron. Astrophys.* **32**, 17

Johnson, H. M.: 1974b, H II Regions and the Galactic Center, 8th ESLAB Symposium, Ed. A. F. M. Moorwood, ESRO SP 105, p. 103

Kazès, I., Le Squéren, A. M., Gadéa, F.: 1975, *Astron. Astrophys.* **42**, 9

Kostjakova, E. B., Saveleva, M. V., Dokuchaeva, C. D., Noskava, R. I.: 1968, IAU Symposium no. 34, Reidel (Holland), p. 317

Lada, C. J., Chaisson, E. J.: 1973, *Astrophys. J.* **183**, 489

Lo, K. Y.: 1974, thesis Mass. Inst. of Technology, Boston (USA)

© European Southern Observatory • Provided by the NASA Astrophysics Data System

1977A&A....59...27I

Lunel, M., Bergeat, J., Sibille, F., Lortet-Zuckermann, M.C.: 1974, *Astron. Astrophys.* **34**, 299
Martin, A.H.M.: 1973, *Monthly Notices Roy. Astron. Soc.* **163**, 141
Matthews, H.E., Goss, W.M., Winnberg, A., Habing, H.J.: 1973, *Astron. Astrophys.* **29**, 309
Meaburn, J.: 1975, H II Regions and Related Topics, Ed. T.L. Wilson and D. Downes, Springer, Heidelberg (BRD), p. 222
Mezger, P.G., Henderson, A.P.: 1967, *Astrophys. J.* **147**, 471
Mezger, P.G., Schraml, J., Terzian, Y.: 1976, *Astrophys. J.* **150**, 807
Minn, Y.K., Greenberg, J.M.: 1975, *Astrophys. J.* **196**, 161
Morris, M., Palmer, P., Turner, B.E., Zuckerman, B.: 1974, *Astrophys. J.* **191**, 349
O'Dell, C.R.: 1963, *Astrophys. J.* **138**, 67
Panagia, N.: 1973, *Astron. J.* **78**, 929
Reifenstein, E.C., Wilson, T.L., Burke, B.F., Mezger, P.G., Altenhoff, W.J.: 1970, *Astron. Astrophys.* **4**, 357
Rydbeck, O.E.H., Kollberg, E., Hjalmarson, A., Sume, A., Elldér, J., Irvine, W.M.: 1975, Research Report no. 120, Chalmers Univ. Gothenburg (Sweden)
Sibille, F., Lunel, M., Bergeat, J.: 1976, *Astron. Astrophys.* **47**, 161, thesis Univers, Claude Bernhard, Lyon (France)
Someren Gréve, H.W. van: 1974, *Astron. Astrophys. Suppl.* **15**, 343
Thaddeus, P., Kutner, M.L., Penzias, A.A., Wilson, R.W., Jefferts, K.B.: 1972, *Astrophys. J. Letters* **176**, L 73
Tucker, K.D., Kutner, M.L., Thaddeus, P.: 1974, *Astrophys. J. Letters* **193**, L 115
Turner, B.E., Gammon, R.H.: 1975, *Astrophys. J.* **198**, 71
Turner, B.E., Zuckerman, B., Palmer, P., Morris, M.: 1973, *Astrophys. J.* **186**, 123
Viotti, R., Nesci, R.: 1974, H II Regions and the Galactic Center, 8th ESLAB Symposium, Ed. A.F.M. Moorwood, ESRO SP 105, p. 19
Wilson, W.J., Schwartz, P.R., Epstein, E.E., Johnson, W.A., Etcheverry, R.D., Mori, T.T., Berry, G.G., Dyson, H.B.: 1974, *Astrophys. J.* **191**, 357
Wink, J.E., Altenhoff, W.J., Webster, W.J.: 1975, *Astron. Astrophys.* **38**, 109
Wynn-Williams, C.G., Becklin, E.E., Neugebauer, G.: 1974a, *Astrophys. J.* **187**, 473
Wynn-Williams, C.G., Werner, M.W., Wilson, W.J.: 1974b, *Astrophys. J.* **187**, 41
Zuckerman, B.: 1973, *Astrophys. J.* **183**, 863

© European Southern Observatory • Provided by the NASA Astrophysics Data System